

2013•2014  
FACULTEIT GENEESKUNDE EN LEVENSWETENSCHAPPEN  
*master in de biomedische wetenschappen*

## Masterproef

Heat transfer resistance as a tool to quantify hybridization efficiency of  
DNA on a nanocrystalline diamond surface

Promotor :  
Prof. dr. Patrick WAGNER

Copromotor :  
dr. Bart VAN GRINSVEN

De transnationale Universiteit Limburg is een uniek samenwerkingsverband van twee universiteiten  
in twee landen: de Universiteit Hasselt en Maastricht University.



Universiteit Hasselt | Campus Hasselt | Martelarenlaan 42 | BE-3500 Hasselt  
Universiteit Hasselt | Campus Diepenbeek | Agoralaan Gebouw D | BE-3590 Diepenbeek

Peter Cornelis

*Proefschrift ingediend tot het behalen van de graad van master in de biomedische  
wetenschappen*



**Maastricht University**

2013•2014  
FACULTEIT GENEESKUNDE EN  
LEVENSWETENSCHAPPEN  
*master in de biomedische wetenschappen*

## Masterproef

Heat transfer resistance as a tool to quantify  
hybridization efficiency of DNA on a nanocrystalline  
diamond surface

Promotor :  
Prof. dr. Patrick WAGNER

Copromotor :  
dr. Bart VAN GRINSVEN

Peter Cornelis

*Proefschrift ingediend tot het behalen van de graad van master in de biomedische wetenschappen*



# Preface

---

Completing this work has been very challenging and I would like to take this opportunity to thank all the people that made it possible.

First of all, I would like to thank Professor Patrick Wagner for believing in my capabilities to successfully complete the bio-electronics and nanotechnology master program and for all his support, guidance and stimulating lectures.

My supervisors, Dr. Bart van Grinsven and Dr. Karolien Bers, also deserve special thanks for their guidance, support and patience under very challenging conditions.

I was very fortunate for being part of the BIOS group at the Institute for Materials Research (IMO). They always provided a relaxed, entertaining and stimulating environment to work in. So thank you very much Thijs, Mohammed, Patricia, Marloes, Evelien, Kathia, Andreas, Kasper, Mehran, Matthias and Yasin.

These last two years studying at Hasselt University have been very memorable thanks to all my wonderful fellow students. Thanks for all those exiting times we spend together. And I would like to specially thank Gideon for being an exceptional colleague these past few months.

And finally, of course, all my family and friends whose support has been instrumental in giving me the strength and persistence to get here.

*In God we trust. All others must bring data.*

**W. Edwards Deming**

*In der Beschränkung Zeigt sich erst der Meister*

**Goethe**



# Table of Contents

---

Preface .....	I
Table of Contents .....	III
List of Symbols and Abbreviations .....	V
Summary .....	VII
Samenvatting .....	VII
Chapter 1: Introduction .....	1
Chapter 2: Materials & Methods .....	7
2.1: Coating of the sensor with nanocrystalline diamond .....	7
2.2: Preparation of the sensor surface for DNA attachment.....	7
2.3: Confocal Laser Scanning Microscopy (CLSM) .....	7
2.4: Attachment of probe DNA to the surface .....	7
2.5: Target hybridization .....	8
2.6: Heat transfer resistance measurement setup.....	8
2.7: Target concentration to effect size ratio .....	8
2.8: Automation .....	9
Chapter 3: Results & Discussion .....	11
3.1: Target concentration to effect size ratio.....	11
3.2: Automation .....	15
Chapter 4: Conclusion.....	21
References .....	23
Supplemental Information .....	25
Articles.....	25



# List of Symbols and Abbreviations

---

<b>ADME</b>	<u>a</u> bsorption, <u>d</u> istribution, <u>m</u> etabolism, <u>e</u> xcretion
<b>CLSM</b>	<u>c</u> onfocal <u>l</u> aser <u>s</u> canning <u>m</u> icroscopy
<b>dsDNA</b>	<u>d</u> ouble <u>s</u> tranded <u>DNA</u>
<b>EDC</b>	1- <u>e</u> thyl-3-[3- <u>d</u> imethylaminopropyl]- <u>c</u> arbodiimide
<b>GUI</b>	<u>g</u> raphical <u>u</u> ser <u>i</u> nterface
<b>HTM</b>	<u>h</u> eat <u>t</u> ransfer <u>m</u> ethod
<b>HTR</b>	<u>h</u> eat <u>t</u> ransfer <u>r</u> esistance ( $R_{th}$ )
<b>IDE</b>	<u>i</u> ntegrated <u>d</u> evelopment <u>e</u> nvironment
<b>JDK</b>	java <u>d</u> evelopment <u>k</u> it
<b>LOD</b>	<u>l</u> imit <u>o</u> f <u>d</u> etection
<b>MES</b>	2-[N- <u>m</u> orpholino]- <u>e</u> thanesulfonic acid
<b>MIP</b>	<u>m</u> olecularly <u>i</u> mprinted <u>p</u> olymer
<b>MPECVD</b>	<u>m</u> icrowave <u>p</u> lasma- <u>e</u> nhanced <u>c</u> hemical <u>v</u> apor <u>d</u> eposition
<b>NCD</b>	<u>n</u> anocrystalline <u>d</u> iamond
<b>NIP</b>	<u>n</u> on <u>i</u> mprinted <u>p</u> olymer
<b>PAH</b>	<u>p</u> henylalanine <u>h</u> ydroxylase
<b>PBS</b>	<u>p</u> hosphate <u>b</u> uffered <u>s</u> aline
<b>PCR</b>	<u>p</u> olymerase <u>c</u> hain <u>r</u> eaction
<b>PDMS</b>	<u>p</u> olydimethylsiloxane
<b>PID</b>	<u>p</u> roportional <u>i</u> ntegral <u>d</u> erivative
<b>rDNA</b>	<u>r</u> ibosomal <u>DNA</u>
<b><math>R_{th}</math></b>	heat transfer resistance (HTR)
<b>SDS</b>	<u>s</u> odium <u>d</u> odecyl <u>s</u> ulphate
<b>SIP</b>	<u>s</u> urface <u>i</u> mprinted <u>p</u> olymer
<b>SNP</b>	<u>s</u> ingle <u>n</u> ucleotide <u>p</u> olymorphism
<b>SSC</b>	<u>s</u> aline <u>s</u> odium <u>c</u> itrate
<b>ssDNA</b>	<u>s</u> ingle <u>s</u> tranded <u>DNA</u>





# Summary

---

This work reports on a label-free real-time method based on heat transfer resistivity for thermal monitoring of DNA denaturation and its potential to quantify DNA fragments with a specific sequence of interest. Determining the contamination level of water for example, is something that could be achieved using this technique. Probe DNA, consisting of a 36-mer fragment, was covalently immobilized on a nanocrystalline diamond surface, created by chemical vapor deposition on a silicon substrate. Various concentrations of full matched 29-mer target DNA fragments were hybridized with this probe DNA. The observation that the change in heat transfer resistance upon denaturation depends on the concentration of target DNA used during the hybridization allowed for the determination of a dose response curve. Therefore, these results illustrate the potential of this technique to quantify the concentration of a specific DNA fragment and to quantify the hybridization efficiency to its probe, which is the percentage of the target DNA exposed to the sensor that is effectively hybridized to the probes. The low hybridization efficiency of around 8 % calculated for the current sensor corresponds with literature. Improving the efficiency could lower the limit of detection of this technique as well as extend the range of concentrations that can be measured. Analysis of the measurement data generated by the setup is a multi-step process that is sensitive to human variability. In order to remove all human error and variability from the analysis process, a software program was developed to automate this task. It not only enhanced the heat transfer method (HTM) used in this study, but also allows for future development of a device that can automatically perform a measurement and generate the corresponding result.

# Samenvatting

---

Dit werk behandelt een label-vrije real-time methode op basis van warmtegeleidingseffecten voor het volgen van DNA denaturatie en het potentieel hiervan om de hoeveelheid DNA fragmenten met een specifieke sequentie te kwantificeren. Met deze techniek is het bijvoorbeeld mogelijk het bacteriële contaminatie niveau van water te bepalen. Probe DNA, met een lengte van 36 baseparen, werd covalent geïmmobiliseerd op een nanokristallijn diamant oppervlak, dat werd gemaakt door chemische dampafzetting op een siliciumsubstraat. Verschillende concentraties van target DNA, met een lengte van 29 baseparen en volledig complementair met de probe DNA sequentie, werden gehybridiseerd met het geïmmobiliseerde probe DNA. Uit de resultaten blijkt dat de verandering die optreedt in de warmtegeleidingsweerstand tijdens de DNA denaturatie afhankelijk is van de concentratie van het target DNA die gebruikt werd om het probe DNA te hybridiseren. Dit liet toe een dosis respons curve hiervoor op te stellen. Hierdoor illustreren deze resultaten het potentieel van deze techniek om niet alleen de hoeveelheid target DNA in een onbekende oplossing te bepalen, maar ook om de efficiëntie te berekenen waarmee het target DNA hybridiseert met het probe DNA. De lage efficiëntie, die voor de huidige sensor berekend werd als zijnde ongeveer 8 %, komt overeen met hetgeen reeds uit de literatuur bekend is voor vergelijkbare oppervlakken. Het verbeteren van de efficiëntie kan de detectielimiet van deze techniek verlagen. Ook het bereik van concentraties die men zou kunnen meten kan hierdoor uitgebreid worden. De analyse van de meetgegevens, die door de methode gegenereerd worden, bestaat uit een aantal stappen waarvan er enkele gevoelig zijn voor de introductie van extra variabiliteit, waarvan de grootte afhankelijk is van de persoon die de analyse uitvoert. Om alle menselijke fouten en de voornoemde variabiliteit uit het analyse proces te verwijderen werd een software programma ontwikkeld om deze taak te automatiseren. Dit verbetert niet alleen de warmteoverdracht methode (HTM) gebruikt in deze studie, maar zet ook de deur verder open naar de ontwikkeling van een toestel dat volledig automatisch een meting kan uitvoeren alsmede het bijhorende resultaat kan berekenen en weergeven.



# Chapter 1: Introduction

A single nucleotide polymorphism (SNP, pronounced snip) is a variation in the DNA sequence that occurs when a single nucleotide in a shared sequence differs between members of the same biological species or paired chromosomes. They occur much more frequently in the non-coding than in the coding part of the genome, because only the coding part is subjected to natural selection which eliminates any non viable mutation. These SNPs are involved in numerous genetic disorders such as Parkinson<sup>(1)</sup>, Alzheimer<sup>(2)</sup>, phenylketonuria<sup>(3)</sup> and several types of cancer.<sup>(4, 5)</sup> When these occur in the genes responsible for regulating the ADME (absorption, distribution, metabolism, excretion) pathway, they can have a profound negative effect on the effectiveness of a treatment. The detection and identification of these SNPs thus plays a very important role in genomic research and theranostics.<sup>(6)</sup> Sequence polymorphisms in the 16S rDNA gene sequence, which is a component of the 30S small subunit of bacterial ribosomes, can be used for bacterial identification<sup>(7)</sup> and the detection of plant pathogens in agriculture<sup>(8)</sup>, bacterial contaminants during food production<sup>(9, 10)</sup> or human pathogens in patients<sup>(11, 12)</sup>.

Because of its outstanding material properties such as high thermal conductivity, chemical inertness and electronic properties, diamond has proven itself as an excellent platform for biomedical research.<sup>(13)</sup> Intrinsic diamond also displays a high chemical and electrochemical stability as well as a wide band gap (5.5 eV).<sup>(14-16)</sup> In recent years, major developments have been made in the field of DNA electrochemical biosensors leading to the development of field-effect sensors<sup>(17-19)</sup> and sensors monitoring electrical surface properties such as impedance<sup>(20)</sup> or capacitance<sup>(21)</sup>. In previous work it was established that monitoring the changes in heat transfer resistance (HTR) of a nanocrystalline diamond (NCD) sample, which was functionalized with specific DNA probes, can reveal information about duplex stability.<sup>(22)</sup> The difference in geometrical configuration between dsDNA (rod-like shape) and ssDNA (sphere-like shape) was hypothesized to be responsible for the change in heat transfer resistance upon denaturation. The persistence length of dsDNA is 50 nm, which is why dsDNA fragments with less than 100 base pairs can be considered as "stiff rods".<sup>(13, 23)</sup> For ssDNA the persistence length drops to 1.48 nm<sup>(23)</sup> causing them to curl up in irregular sphere-like shapes, and their typical Flory radius can be approximated using formula 1.1, where L is the total length of the DNA fragment and  $L_p$  its persistence length.<sup>(13)</sup>

$$r_{Flory} = \sqrt{\frac{L_p * L}{3}} \quad (1.1).$$

During denaturation the DNA fragments immobilized on the surface change from dsDNA to ssDNA causing an increase in their surface coverage, which in turn causes additional hindrance for the solid-to-liquid heat transfer at the sensor surface (Fig. 1.1).

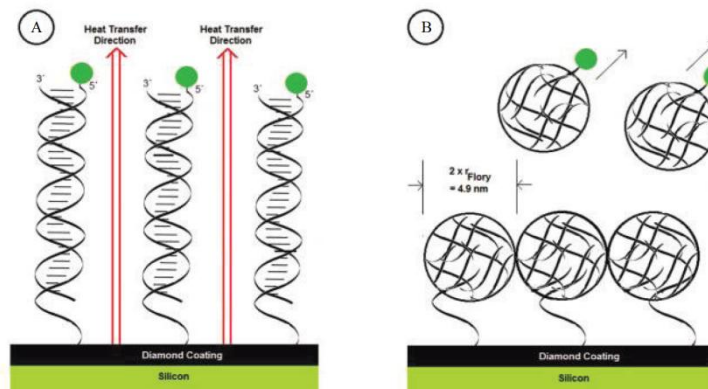


**Fig. 1.1.** Panel A illustrates the heat transfer path through the DNA brush on the sensor surface. After denaturation, the probe curls up, thus hindering the solid-to-liquid heat transfer.<sup>(22)</sup>

# Chapter 1 : Introduction

Thermal stability information received from this technique in the form of melting temperatures was proven to be accurate enough to detect SNPs in target DNA sequences. Mutations decrease duplex stability, which leads to a lower denaturation (melting) temperature of the dsDNA as illustrated in Fig. 1.2.

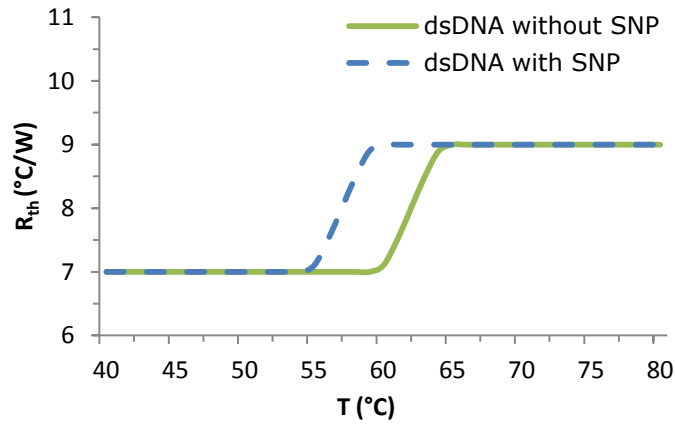


**Fig. 1.2.** Illustration of the increase in heat transfer resistance during temperature ramping of dsDNA with(dashed line) and without(full line) SNP.

In subsequent work, indications for two more functionalities of this method were established.<sup>(24)</sup> First, by only completely covering a certain percentage (25%, 50%, 75%, 100%) of the sensor-surface with dsDNA and leaving the rest single-stranded, a linear relationship between the surface area covered with dsDNA and the change in heat transfer resistance upon denaturation was detected (Fig. 1.3).

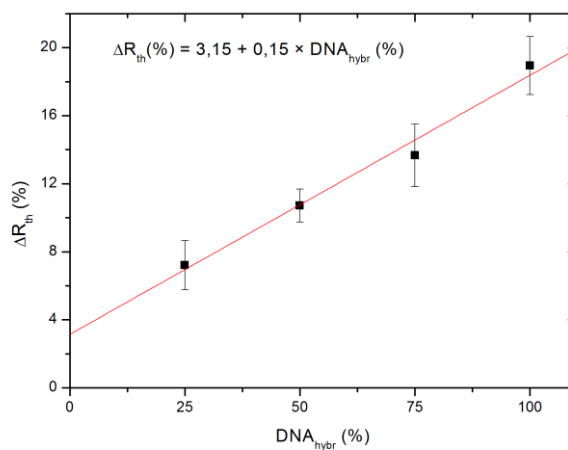


**Fig. 1.3.** Correlation between surface coverage and change in heat transfer resistance. 100 % surface coverage equals 15 mm<sup>2</sup>.

# Chapter 1 : Introduction

Selective surface hybridization was done using a PDMS mold with four equally sized chambers. Fluorescently marked target DNA was used to check the hybridization distribution on the surface (Fig. 1.4). The fluorescent marker used was an Alexa Fluor 488 dye.

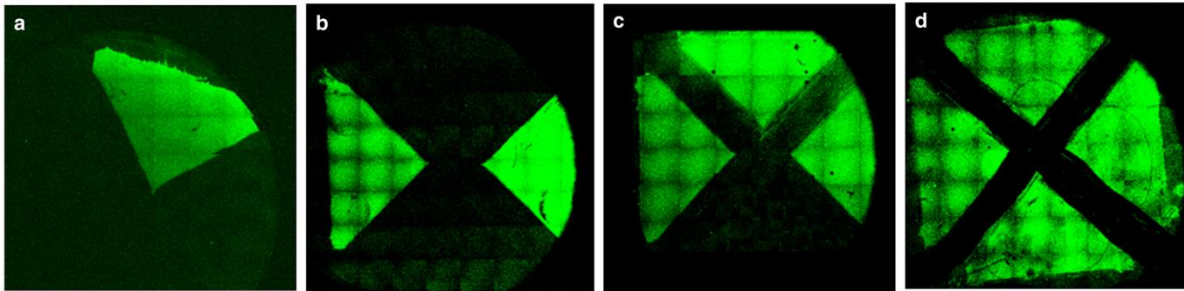


**Fig. 1.4.** Fluorescent images of the sensor surface to confirm target-DNA attachment to specific areas.<sup>(24)</sup> a) 25% surface coverage b) 50% surface coverage c) 75% surface coverage d) 100% surface coverage.

However, no analysis of the response in heat transfer resistance to a complete surface coverage with reduced concentrations of target DNA has been performed. This is very interesting because it might allow determining the concentration of specific DNA sequence of interest in an unknown sample. For example, the contamination level of a sample with a particular strain of bacteria could be determined using this technique by selecting a part of the ribosomal DNA sequence that is unique for that specific strain.

From literature it is also known that when probe DNA is attached to a surface the probe density on that surface has an effect on the hybridization efficiency with the target DNA sequences.<sup>(25)</sup> In order for the target DNA to be able to hybridize with the probes it needs to infiltrate the layer of curled up single stranded probes on the surface. As probe densities increase this gets more difficult because the steric and electrostatic hindrance from neighboring probes increases.<sup>(26, 27)</sup> On the other hand preheating the probe DNA before hybridization increases the efficiency, but only for lower probe densities. Hybridization kinetics in function of probe density can be seen in Fig. 1.5. As such, this effect also needs to be considered when analyzing the response in heat transfer resistance to reduced concentrations of target DNA.

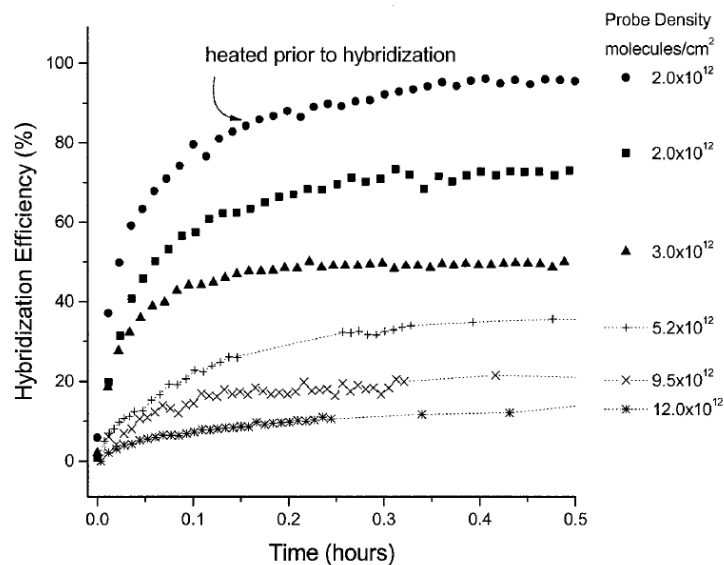


**Fig. 1.5.** Hybridization kinetics as a function of probe density.<sup>(25)</sup> Heating of the probe surface before hybridization increases the efficiency, but only at lower probe densities.

# Chapter 1 : Introduction

Another reason the probe density might affect the change in heat transfer resistance during measurements lies in the difference in surface coverage between the single stranded probe and the double stranded hybridized probe. Ideally the un-hybridized probe DNA should cover 100% of the surface. However, the probe density retrieved from literature of  $8 \times 10^{12}/\text{cm}^2$  multiplied by the surface calculated from the Flory radius results in a theoretical surface coverage of approximately 150%. The spheres of un-hybridized probe should therefore be seen as being intertwined instead of free standing. As such, steric and electrostatic hindrances are increased, thereby lowering the hybridization efficiency (Fig. 1.6). Further analysis of the effect of probe density on HTR measurements is therefore necessary.

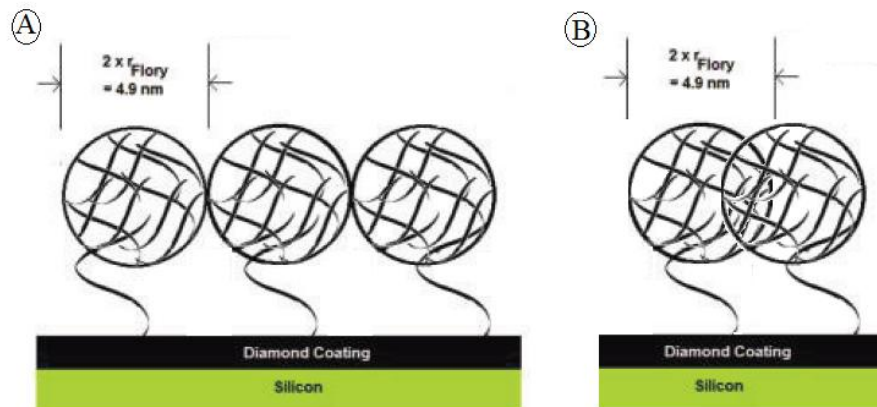


**Fig. 1.6.** Panel A illustrates the ideal situation with all the probes in their single stranded geometrical configuration positioned nicely next to one another. At high probe densities the distance between the individual probes becomes smaller than the diameter of area they occupy on the surface causing them to get intertwined. This increases the steric and electrostatic hindrance the target DNA has to overcome during hybridization (Panel B).

Second, when the melting temperature, which is a measure of duplex stability between a normal gene fragment and its mutated form, is significantly different, they could be detected simultaneously as a bipartite change in heat transfer resistance upon temperature ramping when both forms are hybridized on distinct regions of the NCD sample (Fig. 1.7).

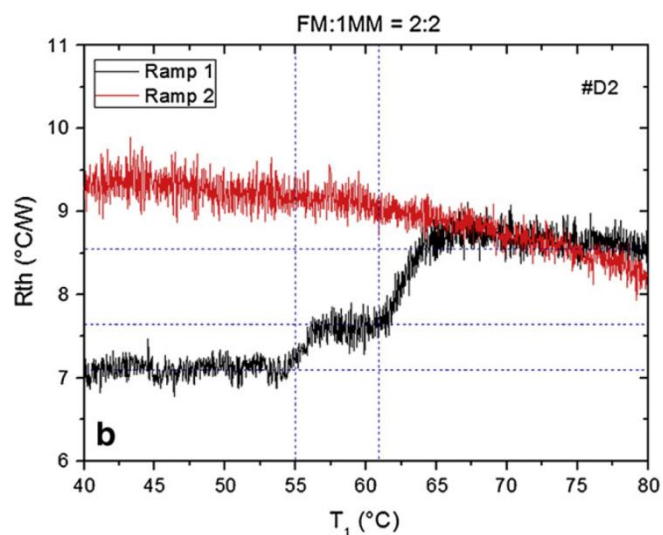


**Fig. 1.7.** Example of a bipartite change in heat transfer resistance. In this case one half of the sensor surface was hybridized with target DNA containing no mutations while the other half was hybridized using target DNA containing a SNP. Denaturing of the DNA sequence with a SNP is responsible for the first rise in  $R_{th}$  while the second rise is caused by the denaturation of the DNA sequence without mutations.

## Chapter 1 : Introduction

Spatial separation of the hybridization was done using the same PDMS mold that was used for selective surface hybridization. Two similarly fluorescently marked target DNA fragments, one normal and one with a SNP, were used (Fig. 1.8). The exact position of the SNP within the DNA sequence has a small effect on its melting temperature, but this is so small that it is difficult to distinguish between two sequences with a SNP at different positions.<sup>(22)</sup> The results of the heat transfer resistance measurements of these surfaces showed the ratios of both parts of the bipartite change in  $R_{th}$  corresponding well to the ratios of hybridized target sequences. However, further analysis is required to evaluate this for heterogeneously hybridized mixtures of mutated and non-mutated gene fragments.

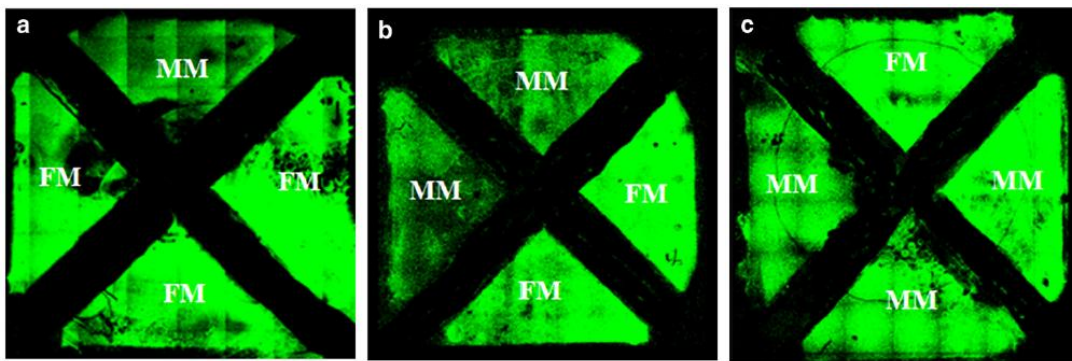


**Fig. 1.8.** Fluorescent images of selectively hybridized NCD samples with full matching target DNA (FM) and target DNA with a SNP (MM).<sup>(24)</sup> a) 1MM:3FM b) 2MM:2FM c) 3MM:1FM

Analyzing the effect of lowering the concentration of target DNA on the change in heat transfer resistance and calculating the hybridization efficiency will be the main focus of this study and allow obtaining a dose-response curve. The DNA sequence that was chosen in previous work is the exon-9 fragment of the phenylalanine hydroxylase (PAH) gene.<sup>(22, 24)</sup> Mutations in this gene can lead to the metabolic disorder phenylketonuria.<sup>(3)</sup> The same sequence is used during this research for easy comparison with the results from previous studies. This provides additional checkpoints to verify the results of this study.



# Chapter 1 : Introduction

# Chapter 2: Materials & Methods

---

## *2.1: Coating of the sensor with nanocrystalline diamond*

Doped (10-20k $\Omega$ cm) 10 x 10 mm<sup>2</sup> p-type crystalline silicon wafers (100) were seeded with a water-based colloid of ultra-dispersed detonation (nano)diamond. On this silicon substrate, nanocrystalline diamond films with thicknesses of ~300 nm and grain sizes of 100 nm were grown using microwave plasma-enhanced chemical vapor deposition (MPECVD) in an ASTEX reactor equipped with a 2.45 GHz microwave generator. This was achieved using a standard mixture of 15 sccm methane gas (CH<sub>4</sub>) and 485 sccm hydrogen gas (H<sub>2</sub>) under a pressure of 45 Torr (60 hPa) and a temperature of 750 °C, with the microwave power set to 4000 W. Under these conditions, the growth rate is ~390 nm/h.

## *2.2: Preparation of the sensor surface for DNA attachment*

The diamond surface was hydrogenated at 700 °C during 30 s at 3500 W under a pressure of 12 kPa and an atmosphere of 1000 sccm hydrogen gas (H<sub>2</sub>).<sup>(28)</sup> Covalent attachment of the amino-modified probe DNA using the zero-length linker 1-ethyl-3-[3-dimethylaminopropyl]-carbodiimide (EDC) requires a carboxyl (COOH) terminated surface. For this purpose, the hydrogen terminated diamond surface was covered with a thin film of unsaturated fatty acid (10-undecenoic acid) under inert atmosphere and covered with a quartz-glass slide before being exposed to UV radiation (254 nm, 265 mW/cm<sup>2</sup>) for 20 h. The carbon-carbon double bond of the unsaturated fatty acid chain breaks and a covalent bond with the hydrogen terminated diamond is established. This photochemical grafting technique is presumably mediated by photoemission from the surface.<sup>(16, 29)</sup> The remaining unbound fatty acid was washed off using acetic acid at 120 °C and warm milliQ water. The thickness of the resulting fatty acid layer is about 2 nm.<sup>(30)</sup>

## *2.3: Confocal Laser Scanning Microscopy (CLSM)*

Fluorescence images for intensity studies and photobleaching experiments were taken using a Zeiss LSM 510 META Axiovert 200 M laser scanning confocal fluorescence microscope. To excite the Alexa Fluor 488 dye, used to label the DNA, an argon-ion laser with a wavelength of 488 nm was used. The maximum intensity at the sample surface was restricted to 30  $\mu$ W to avoid bleaching during image acquisition. This is achieved by using a pinhole size of 150  $\mu$ m and a laser intensity of 10 %. The peak emission of the dye is 518 nm, which is longer than expected due to vibrational relaxation of the molecule after photon absorption. A 10 x 0.3 Plan Neofluar air objective with a working distance of 5.6 mm was used to collect all images. The detector gain, which is a measure for the photomultiplier voltage in arbitrary units, was set to 950. To confirm that the fluorescence originated from the Alexa Fluor 488 dye, photobleaching experiments were done. A small region on the surface was exposed to a laser intensity of 100 % for a few minutes and afterwards a new image was collected using the standard settings. ImageJ software from National Institutes of Health (USA) was used to analyze all images.

## *2.4: Attachment of probe DNA to the surface*

The selected probe was a 36-mer single stranded DNA (ssDNA) amino-modified at its 5' end (3'-CCA AGC CCC CAT ATG TAC CCG ACG TCC CC - A AAA AAA C<sub>6</sub>H<sub>12</sub>-NH<sub>2</sub>-5'). Covalent coupling to the carboxyl-terminated surface was done using the zero-length linker EDC in a 2-[N-morpholino]-ethanesulfonic acid (MES) buffer (pH 6) at 4 °C for 2 hours.<sup>(15)</sup> Unbound probe DNA was removed in three washing steps. In the first and second step, the sample was washed with phosphate buffered saline (1x PBS) of pH 7.2 for 5 minutes. Third, the sample was washed with 2x saline sodium citrate (SSC) with 0.5 % sodium dodecyl sulphate (SDS) for 30 minutes. Finally, the sample was rinsed with a 1x PBS solution before being stored in 1x PBS at 4 °C.

## Chapter 2 : Materials & Methods

### 2.5: Target hybridization

First, 6  $\mu\text{l}$  of a selected sample of target DNA was added to 14  $\mu\text{l}$  1x PCR buffer, 20  $\mu\text{l}$  of this mixture was used to cover the complete NCD sample. In the next step, the sample was incubated at 35  $^{\circ}\text{C}$  for 2 h to allow hybridization to take place. During hybridization, the sample was kept under saturated water vapor atmosphere to avoid evaporation of the reaction liquid. Any non-specifically bound target DNA was removed in two washing steps. Therefore, the sample was first washed with 2x SSC + 0.5 % SDS for 30 minutes. Subsequently, the sample was washed with 0.2x SSC at 30  $^{\circ}\text{C}$  for 5 minutes and with 0.2x SSC at room temperature for 5 minutes. Finally, the sample was rinsed with 1x PBS of pH 7.2 and stored in PBS at 4  $^{\circ}\text{C}$ .<sup>(14)</sup> To avoid denaturation of newly formed dsDNA during washing, a low salt concentration in comparison to the hybridization buffer and a washing temperature of 5  $^{\circ}\text{C}$  below the hybridization temperature were used.

### 2.6: Heat transfer resistance measurement setup

The general principle of the heat transfer method (HTM) is shown in Fig. 2.1. The whole system centers around an adjustable heat source attached to a copper block. The heat source transfers a thermal current through a NCD chip (1  $\text{cm}^2$ ) that was attached to the copper block using a very thin layer of conductive silver paste. This whole assembly was then screwed to the flow cell using a rubber O-ring separator to achieve a good seal between the NCD chip and the liquid chamber. The contact area between the chip and the liquid compartment was 28  $\text{mm}^2$ . The temperature of the copper block,  $T_1$ , was stringently controlled during the measurement using a PID controller ( $P=1$ ,  $I=8$ ,  $D=0.1$ ) while the temperature in the liquid beneath the NCD chip,  $T_2$ , was monitored. Also the voltage applied to the heat source, needed to keep  $T_1$  at the programmed temperature, was recorded. The heating power,  $P$ , can be calculated by dividing the squared voltage by the resistance of the heat source (22  $\Omega$ ). From the temperature difference  $T_1 - T_2$  and the heating power  $P$ , the heat transfer resistance can be derived from  $R_{\text{th}} = (T_1 - T_2)/P$ .<sup>(31, 32)</sup>

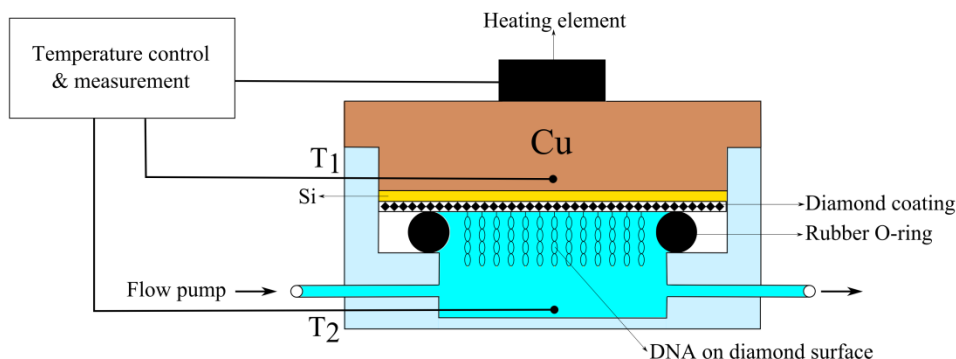


**Fig. 2.1.** Schematic layout of the measurement setup, allowing for the monitoring of DNA denaturation by measuring the heat transfer resistance. Probe DNA is covalently immobilized on a diamond-coated silicon substrate. The cell is filled with 1x PBS buffer. A thermocouple is used to measure the temperature of the copper ( $T_1$ ), which can be actively controlled using a PID-controller ( $P=1$ ,  $I=8$ ,  $D=0.1$ ). The liquid temperature ( $T_2$ ) is measured by a second thermocouple. The parameters needed to calculate the heat transfer resistance are the temperature difference  $T_1 - T_2$  and the input power  $P$  provided by the heating element.

### 2.7: Target concentration to effect size ratio

The selected target fragment was a 29-mer single stranded DNA modified with Alexa Fluor 488 at its 5' end (5'-GGT TCG GGG GTA TAC ATG GGC TGC AGG GG-3'). Four different concentrations were used to determine a dose-response curve. The concentration of target DNA in the stock solution was similar to that in previous work (100  $\text{pmol}/\mu\text{l}$ ).<sup>(22, 24)</sup> This stock solution was diluted respectively 5, 10 and 20 times. The range of concentrations used is thus 100  $\text{pmol}/\mu\text{l}$ ,

## Chapter 2 : Materials & Methods

20 pmol/ $\mu$ l, 10 pmol/ $\mu$ l and 5 pmol/ $\mu$ l. For each concentration, the change in heat transfer resistance upon temperature ramping was measured. At the start of the measurement,  $T_1$  was held constant at 35 °C while during the measurement it was increased to 85 °C at a rate of 1 °C/min and decreased at the same rate to 35 °C by changing the heating power accordingly. This heating/cooling cycle was performed two consecutive times.

### *2.8: Automation*

The measurement setup generates a single file containing all the data from the measurement. This is a simple text-file with a separate line for every recorded second. Each line contains a timestamp (number of seconds since the measurement started), set temperature (requested temperature for the copper block (°C)), current temperature of the copper block  $T_1$  (°C), current temperature for four different channels (1-4) (°C) and the applied voltage over the thermal resistor (V). In this setup, temperature  $T_2$  is recorded on channel 1.

Analysis is a multi-step process. First, the decimal format of the data is checked and when necessary converted to the correct format for further analysis. In a next step subsets (time slices) of the data, containing a temperature ramp from 40 °C to 80 °C, are extracted. The first two datasets are then selected for further calculations. For each point in the datasets, the heat transfer resistance is calculated using the formulas described in section 2.6. Then, both datasets are plotted on a graph with  $T_1$  (°C) on the x-axis and  $R_{th}$  (°C/W) on the y-axis. The melting temperature of the DNA fragment is determined by averaging the copper temperature  $T_1$  when denaturation of the hybridized DNA starts and ends. Both points are determined visually. The inflection point in the graph of the first dataset represents the beginning of DNA denaturation, while the intersection point of the graphs of both datasets determines the end. The average  $R_{th}$  before and after denaturation is used to calculate the change in  $R_{th}$  as a percentile increase compared to the baseline and as an absolute value.

Manual analysis of the data introduces small supplementary variations in the results that vary in magnitude depending on the person doing the analysis. Automating the analysis removes these variations allowing for a more reliable way to compare the results of different measurements independent of who did the analysis and when. To this end, a software program was developed. Based on elaborate past experience java (JDK version 1.7) was chosen as the programming language for the development. An additional benefit of using java is cross-platform compatibility, which means it can run unaltered on PC's, Mac's and Linux machines. The free open source library JFreeChart (version 1.0.17) was used to display and save graphs. The standard Eclipse IDE for java developers (Kepler service release 1) was used as the development environment.

## Chapter 2 : Materials & Methods

# Chapter 3: Results & Discussion

---

## 3.1: Target concentration to effect size ratio

The goal of this experiment was to analyze the effect of varying the concentration of target DNA on the change in heat transfer resistance upon denaturation. Hybridizing the probe DNA to solutions containing a decreasing amount of target DNA allowed for the determination of a dose-response curve. Before measurement the presence of target DNA on the surface was confirmed using confocal laser scanning microscopy (CLSM). Photobleaching allowed identifying the target DNA as the source of the fluorescence (Fig. 3.1).

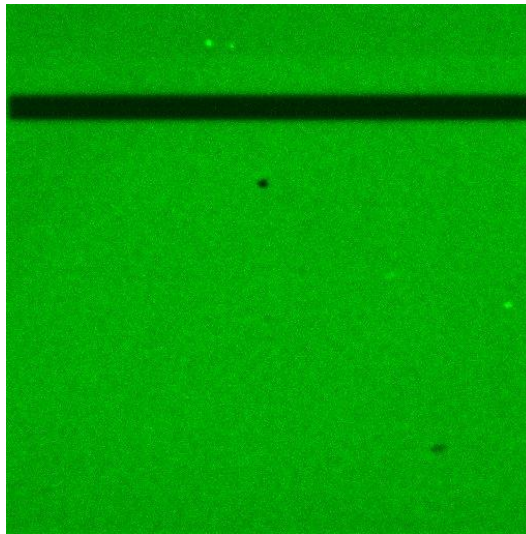


**Fig. 3.1.** Fluorescent image of the sensor surface after hybridization with target DNA. The black area is the result of photobleaching, which removed all fluorescence from the target DNA in that area.

The heat transfer resistance as a function of  $T_1$  is shown in Fig. 3.2 for all concentrations (data has not been filtered). The initial  $R_{th}$  of the double stranded DNA for the undiluted concentration (black line) is around  $7.23 \text{ }^\circ\text{C/W} \pm 0.07 \text{ }^\circ\text{C/W}$  which increases to around  $8.56 \text{ }^\circ\text{C/W} \pm 0.16 \text{ }^\circ\text{C/W}$  upon denaturation at its inflection point at a temperature of  $60.5 \text{ }^\circ\text{C} \pm 0.1 \text{ }^\circ\text{C}$ . In case of the 5x diluted concentration (red line), the initial  $R_{th}$  is around  $7.57 \text{ }^\circ\text{C/W} \pm 0.06 \text{ }^\circ\text{C/W}$  and increases to around  $8.81 \text{ }^\circ\text{C/W} \pm 0.05 \text{ }^\circ\text{C/W}$  at its inflection point at an identical temperature of  $60.5 \text{ }^\circ\text{C} \pm 0.1 \text{ }^\circ\text{C}$ . Hybridizing the surface using the 10x diluted concentration (blue line) results in an initial  $R_{th}$  value of  $8.04 \text{ }^\circ\text{C/W} \pm 0.07 \text{ }^\circ\text{C/W}$  that increases to  $8.67 \text{ }^\circ\text{C/W} \pm 0.04 \text{ }^\circ\text{C/W}$  upon denaturation. Finally, with the 20x diluted concentration (green line) one can find an initial  $R_{th}$  value around  $8.54 \text{ }^\circ\text{C/W} \pm 0.06 \text{ }^\circ\text{C/W}$  which increases to around  $8.73 \text{ }^\circ\text{C/W} \pm 0.05 \text{ }^\circ\text{C/W}$ . The  $R_{th}$  inflection point for these last two concentrations is also at an identical temperature of  $60.5 \text{ }^\circ\text{C} \pm 0.1 \text{ }^\circ\text{C}$ . These results are summarized in Table 3.1.

## Chapter 3 : Results & Discussion

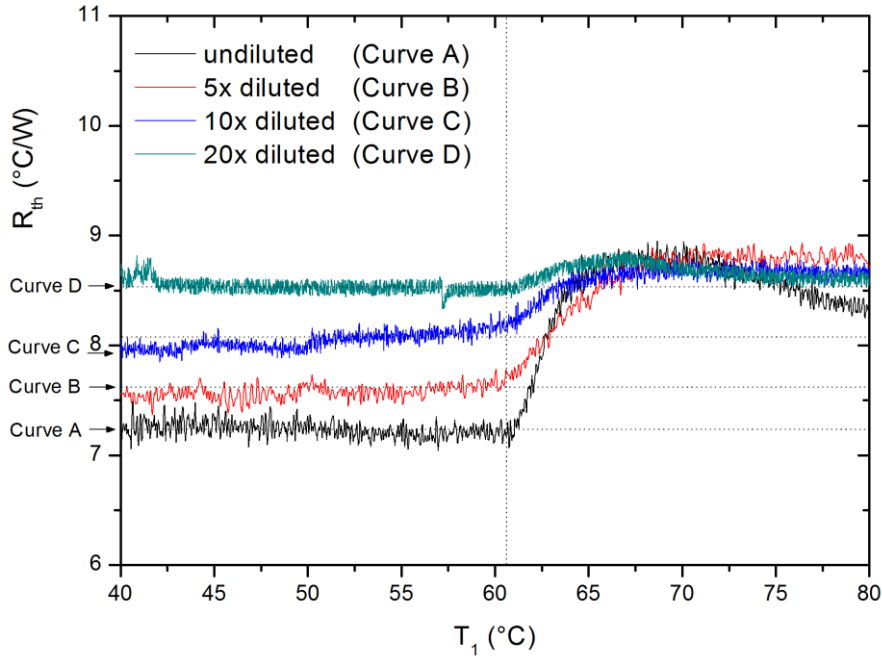


**Fig. 3.2.** Heat transfer resistance as a function of temperature when the NCD is hybridized with a 100 pmol/ $\mu$ l (undiluted), 20 pmol/ $\mu$ l (5x diluted), 10 pmol/ $\mu$ l (10x diluted) and 5 pmol/ $\mu$ l (20x diluted) concentration of target DNA.

**Table 3.1.** Results for the heat transfer measurements using four different dilutions of target DNA.

Dilution	Undiluted	5x	10x	20x
<b>Initial <math>R_{th}</math> (<math>^{\circ}</math>C/W)</b>	$7.23 \pm 0.07$	$7.57 \pm 0.06$	$8.04 \pm 0.07$	$8.54 \pm 0.06$
<b>End <math>R_{th}</math> (<math>^{\circ}</math>C/W)</b>	$8.56 \pm 0.16$	$8.81 \pm 0.05$	$8.67 \pm 0.04$	$8.73 \pm 0.05$
<b>Inflection point (<math>^{\circ}</math>C)</b>	$60.5 \pm 0.1$	$60.5 \pm 0.1$	$60.5 \pm 0.1$	$60.5 \pm 0.1$

The results show that the heat transfer resistance increases as the NCD samples are hybridized with lower concentrations of target DNA. This can be explained by an increase in the amount of probe DNA that is still in its single stranded form after hybridization. It was previously reported that ssDNA has a higher heat transfer resistance in comparison to dsDNA when attached to a surface.<sup>(22)</sup> This difference was hypothesized to be caused by a difference in geometrical configuration, where ssDNA has a spherical shape as opposed to dsDNA, which has a rod-like shape. The persistence length for DNA is 50 nm when double stranded and drops to 1.48 nm when single stranded.<sup>(13, 23)</sup> The fragment length of the target DNA used in these experiments was 29 base pairs, which corresponds to a length of approximately 10 nm. Denaturation causes a conversion of dsDNA to ssDNA and, as such, explains the increase in heat transfer resistance around the melting temperature of the selected probe DNA sequence. As a consequence, lower changes in heat transfer resistance correspond to a lower amount of hybridization on the sample. The effect size of the change in heat transfer resistance ( $\Delta R_{th}$  (%)) can be calculated using Formula 3.1, where  $R_{th(40-60\text{ }^{\circ}\text{C})}$  and  $R_{th(70-80\text{ }^{\circ}\text{C})}$  are the average heat transfer resistance before and after denaturation respectively. The heat transfer resistance after denaturation is the same for all target DNA concentrations because from that point on only ssDNA is present on the sensor surface. This can be clearly seen in Fig. 3.2 where the graphs coincide for temperatures above 65  $^{\circ}$ C.

$$\Delta R_{th} (\%) = ((R_{th(70-80\text{ }^{\circ}\text{C})} - R_{th(40-60\text{ }^{\circ}\text{C})}) / R_{th(40-60\text{ }^{\circ}\text{C})}) \times 100 \quad (3.1)$$

## Chapter 3 : Results & Discussion

The calculated effect sizes for the different concentrations were respectively  $20.83 \pm 0.37 \%$  (undiluted),  $15.79 \pm 0.49 \%$  (5x diluted),  $7.41 \pm 0.43 \%$  (10x diluted) and  $3.57 \pm 0.29 \%$  (20x diluted). These values were plotted on the correlation graph between the amount of hybridization surface coverage ( $\text{DNA}_{\text{hybr}}$ ) and the size of the change in heat transfer resistance obtained from the previous study<sup>(24)</sup>, which can be seen in Fig. 3.3. Looking at this, one can clearly see that the changes in target concentration do not correspond to equal linear changes in the expected hybridization surface coverage necessary to achieve the same effect size. For instance, going from a concentration of 10 pmol/ $\mu\text{l}$  to 20 pmol/ $\mu\text{l}$  results in a bigger change than going from a concentration of 20 pmol/ $\mu\text{l}$  to 100 pmol/ $\mu\text{l}$ . In short, using this method to measure DNA concentrations is not as straightforward as it appeared to be. Other effects might start playing a significant role when the probes on the sensor surface are hybridized with diluted concentrations of target DNA. For example, the electrostatic interference of ssDNA probes surrounding a hybridized dsDNA probe.

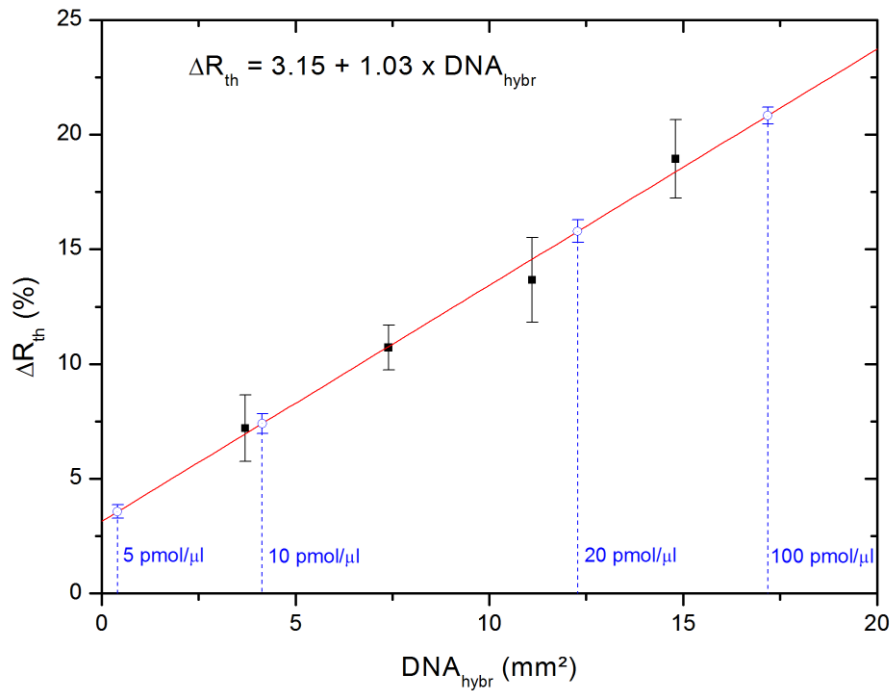


**Fig. 3.3.** Black full boxes and line show the correlation between the amount of hybridization surface coverage ( $\text{DNA}_{\text{hybr}}$ ) and the size of the change in heat transfer resistance.  $\text{DNA}_{\text{hybr}}$  is the area of the surface that is maximally hybridized with target DNA while the rest of the surface only contains un-hybridized single stranded probe DNA. Blue open circles with corresponding concentrations are the current results plotted on the same line to determine the corresponding surface coverage necessary to achieve the same effect size.

Fig. 3.4 shows the dose-response curve that was constructed using the concentration-dependent results and an exponential fit (Equation 3.2), with  $\text{DNA}_{\text{conc}}$  in pmol/ $\mu\text{l}$ .

$$\Delta R_{\text{th}} (\%) = 20.97 - 25.04 \times \exp(-\text{DNA}_{\text{conc}} / 14.28); R^2 = 0.98 \quad (3.2)$$

A linear relationship exists for concentrations between 5 pmol/ $\mu\text{l}$  and 20 pmol/ $\mu\text{l}$ . However, at values above 20 pmol/ $\mu\text{l}$  the  $R_{\text{th}}$  signal starts to saturate, indicating that all available probe DNA fragments are hybridized with target DNA. Further increasing the concentration of DNA will not increase the amount of DNA duplexes prior to denaturation and will therefore not cause an increase in effect size. As a consequence, the DNA concentration in unknown samples must stay below this limit in order to be reliably measured by HTM.



## Chapter 3 : Results & Discussion

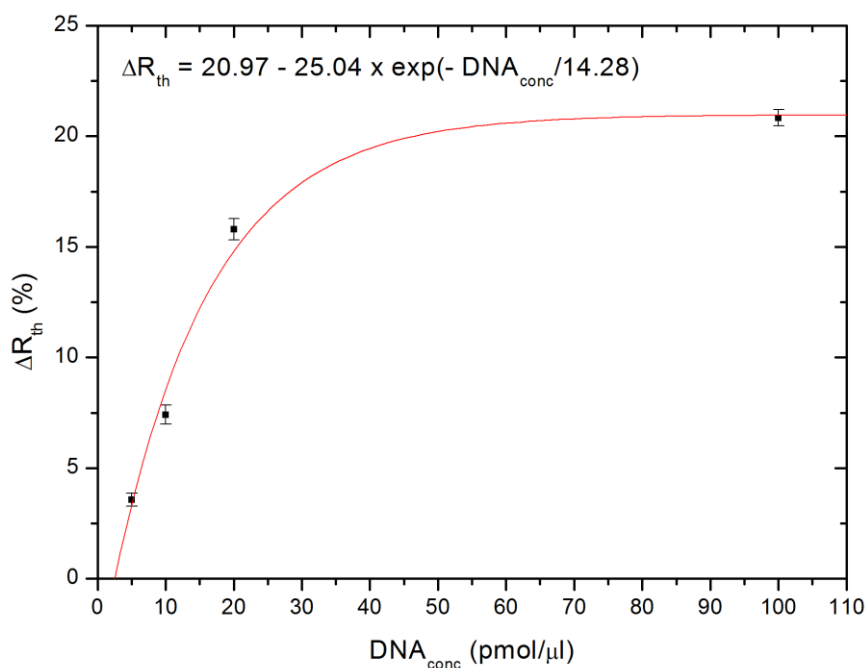


**Fig. 3.4.** Dose-response curve: Change in heat transfer resistance plotted against the target DNA concentration. The solid line was calculated using an exponential fit algorithm.

Expanding the curve to lower concentrations shows that a minimum concentration of 4 pmol/μl is required to be able to detect a change in heat transfer resistance. This was calculated by determining the intersection point between the curve and the limit of detection (LOD), which was set at three times the standard deviation on the measurements. Optimizing the signal-to-noise ratio might enhance the measurement range in the future. This could be achieved by optimizing the PID parameters of the setup. However, further optimization of the NCD sample surface functionalization is definitely necessary to allow this method to be used for concentration measurements. Peterson *et al.* already demonstrated that the probe density on a surface influences the hybridization efficiency.<sup>(25)</sup> The probe density on the NCD samples used in this study is  $8 \times 10^{12}$  probes/cm<sup>2</sup>. The calculated hybridization efficiency (Formula 3.3) for the different concentrations of target DNA is shown in Table 3.2. The average efficiency in the range that is usable for concentration measurements is  $7.95 \pm 3.75$  %. In the study of Peterson *et al.* a different substrate and linker were used to attach DNA probes to the surface, which has an effect on the efficiency of the system. Keeping that in mind, the hybridization efficiency that was measured for the probe density used in this study is comparable in both studies. Lowering the density to  $2 \times 10^{12}$  probes/cm<sup>2</sup> and preheating before hybridization, as proposed by Peterson *et al.*, could therefore significantly improve the hybridization efficiency.

$$\text{Hybridization efficiency (\%)} = (\text{Signal strength (\%)} / ((\# \text{targets} / \# \text{probes}) * 100)) * 100 \quad (3.3)$$

**Table 3.2.** Calculated hybridization efficiencies for the different concentrations of target DNA.

Target concentration (pmol/μl)	100	20	10	5
# targets	$3.61 \times 10^{14}$	$7.23 \times 10^{13}$	$3.61 \times 10^{13}$	$1.81 \times 10^{13}$
# probes	$8 \times 10^{12}$	$8 \times 10^{12}$	$8 \times 10^{12}$	$8 \times 10^{12}$
target/probe	45.17	9.03	4.52	2.26
Signal strength (%)	100	$75.80 \pm 2.71$	$35.57 \pm 2.16$	$17.14 \pm 1.43$
ΔR <sub>th</sub> (%)	$20.83 \pm 0.37$	$15.79 \pm 0.49$	$7.41 \pm 0.43$	$3.57 \pm 0.29$
Efficiency (%)	2.21	$8.39 \pm 2.71$	$7.88 \pm 2.16$	$7.59 \pm 1.43$

## Chapter 3 : Results & Discussion

Steric hindrance at high concentrations, in combination with the electrostatic repulsion caused by the negatively charged DNA backbones, is a likely explanation for the reduction in hybridization efficiency at high probe densities. High target concentrations might even increase these effects to the point where there is so much competition between the different target sequences that sometimes neither gets hybridized to the probe on the surface.

### *3.2: Automation*

The programs functionality is distributed over three main parts. The data processing classes take care of importing and analyzing the data and exporting the results of the analysis. The graphical user interface (GUI) sends the requests from the user to the data processing classes, displays the results and allows the user to export the graphs. The control panel is a separate part of the GUI that manages the specific settings used for data analysis as well as enabling customization of the graphs displayed in the GUI.

Data processing consists of a general module responsible for importing the data from the measurement and a specialized module, which contains analyser modules for every type of analysis available in the program. At the moment, only analysis of DNA denaturation runs is incorporated. In the future this could easily be expanded to include more types of heat transfer measurements. The specialized modules allow exporting the results of the analysis in a standard text-file. The general module is responsible for importing the measurement data and organizing it for efficient further analysis. It also automatically converts the decimal format of the data when necessary, thereby removing the need for pre-processing the measurement data.

The GUI contains four sheets. The first sheet ("About") displays general information about the program (version number, date, ...) (Fig. 3.5). Using the second sheet ("DNA") the different runs of a DNA denaturation experiment can be analyzed (Fig. 3.6). Statistical information like the average, variance and standard deviation is available. For the  $R_{th}$  calculations, the noise level is also calculated and displayed. Finally, by comparing the first two cycles of temperature ramping, the melting temperature and the change in  $R_{th}$  upon denaturation are calculated and displayed. The melting temperature is the average of the copper temperature where DNA denaturation starts and the copper temperature where the denaturation is completed. The change in  $R_{th}$  is calculated in percent as well as in absolute value compared to the start of the first temperature ramp cycle. The calculated  $R_{th}$  values for the selected channels and runs are displayed in a graph along with several options to customize the graph to personal preference. It is also possible to display the complete temperature profile (Fig. 3.7) of all the channels during the entire measurement allowing the detecting of anomalies in the temperature regulation of the setup. The decrease in the temperature ramping speed of the liquid, which signifies an increase in heat transfer resistance, is clearly visible in the shown example and coincides perfectly with the melting temperature of the hybridized DNA on the sensor surface. On the last sheet ("Settings") several parameters of the programs can be adjusted (Fig. 3.8). The default folder for importing data and exporting graphs and results can be set. The resistance of the heating transistor, which is used for calculating the  $R_{th}$ , can be changed to match the actual resistance of the resistor used in the measurement setup. It is also possible to select the channels and heating runs that will be automatically displayed after data import. Finally, also the colors used for the different channels and heating runs can be adjusted to suit ones personal preference.

## Chapter 3 : Results & Discussion



**Fig. 3.5.** About sheet of the Rth-Analyser program.

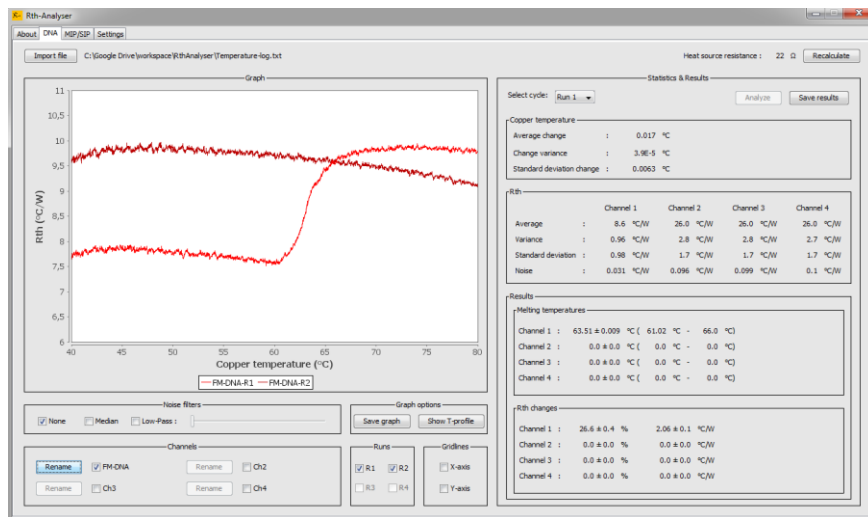


**Fig. 3.6.** DNA sheet of the Rth-Analyser program. As an example the analyses of a NCD surface with  $8 \times 10^{12}$  probes/cm<sup>2</sup> hybridized with a 100 pmol/μl target DNA concentration is shown.

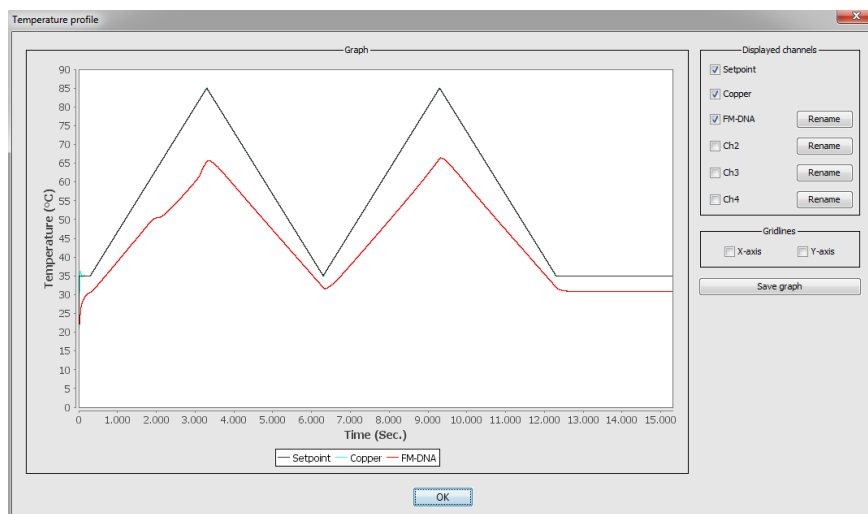


**Fig. 3.7.** Temperature profile of the measurement in Fig. 3.6. The drop in liquid temperature ramping, due to DNA denaturation causing an increase in heat transfer resistance, in the first cycle is clearly visible.

## Chapter 3 : Results & Discussion

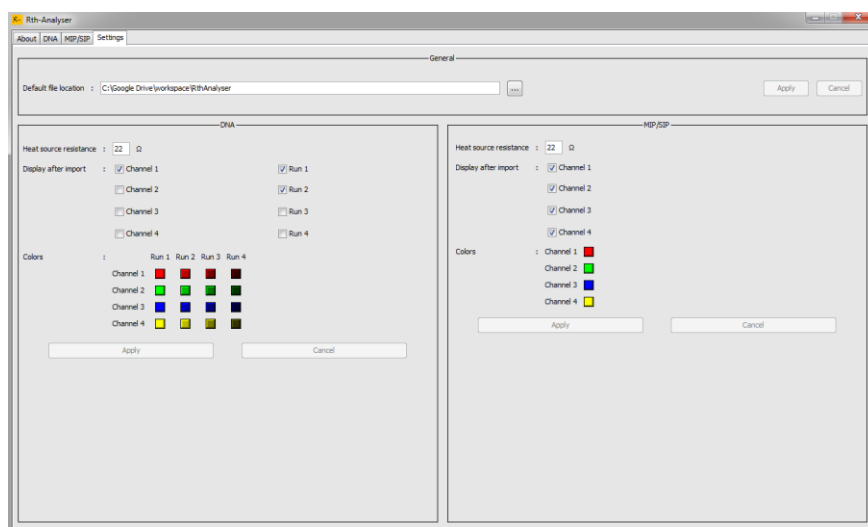


**Fig. 3.8.** Settings sheet of the Rth-Analyser program. Allows adjusting the resistance of the heating transistor to match the actual resistor used in the setup. Several other parameters allow altering the program to suit ones personal preference.

The heat transfer method can also be used in conjunction with two alternative sensors, MIPs and SIPs. MIPs are molecularly imprinted polymers that contain cavities on their surface which can specifically bind a small organic molecule like for instance histamine.<sup>(33)</sup> Upon binding the target molecule the total heat transfer resistance of the polymer increases. The change in heat transfer resistance is a measure for the concentration of target molecule in the solution the sensor is exposed to. SIPs are surface imprinted polymers. Their working principle is similar to MIPs, but they allow the specific detection of larger objects like cells. For instance specific types of cancer cells can be detected using these sensors in combination with the heat transfer method.<sup>(34)</sup>

The change in heat transfer resistance in the case of DNA is caused by a conformational change upon temperature ramping (Fig. 3.9), whereas binding of a specific target to the surface is responsible in the case of MIPs (Fig. 3.10) and SIPs (Fig. 3.11). Measurements with MIPs and SIPs can therefore be conducted at constant temperature, for instance 37.00 °C, to mimic body temperature.

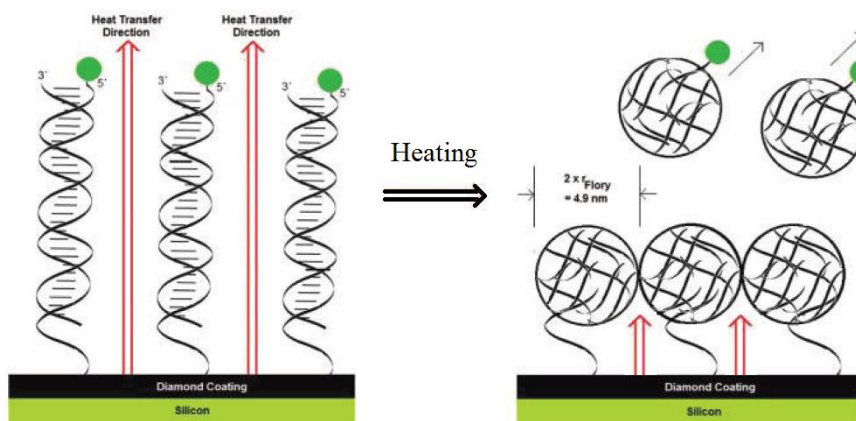


**Fig. 3.9.** Schematic representation of the working principle of the HTM with DNA.<sup>(22)</sup> Upon heating the dsDNA denatures causing a conformational change that increases the thermal resistance of the surface.

## Chapter 3 : Results & Discussion

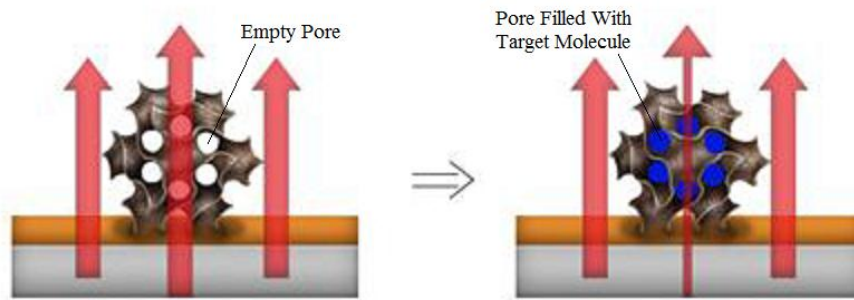


**Fig. 3.10.** Artist's impression of the "pore-blocking model".<sup>(33)</sup> The MIP particles are embedded in the surface and contain several pores with binding sites for its target molecule. When these pores are filled by target molecules, as indicated by the blue dots, heat transfer resistance through the MIP layer is strongly increased.

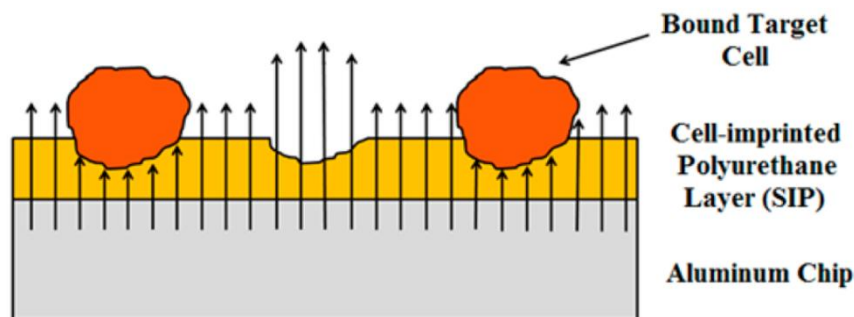


**Fig. 3.11.** Illustration of cell binding to the binding cavities present on the surface of the SIP.<sup>(34)</sup> Binding of a target cell to a cavity increases the heat transfer resistance by blocking the heat transfer from chip to liquid.

Measurements using MIPs or SIPs are done at a constant temperature  $T_1$  and over a set period of time. In both cases a non imprinted polymer (NIP), which has no specific binding sites for the target, can be used to compensate for non-specific absorption of the targets to the surface by subtracting its  $R_{th}$  values from the MIP/SIP results. It starts with exposing the sensor to a buffer solution to determine the base heat transfer resistance value for the sensor and measurement setup. After that, at defined intervals, solutions containing increasing concentrations of targets or an unknown concentration of target are exposed to the sensor surface. At the moment of injection temperature  $T_2$  (liquid temperature) is disturbed, because the injected liquid has a different temperature compared to liquid it replaces in the flow cell, causing spikes in the calculated  $R_{th}$  values. Therefore, after each injection some stabilization time needs to be taken into account. The third sheet ("MIP/SIP") of the program allows displaying the evolution of the  $R_{th}$  values as a function of time for up to four channels simultaneously, thus allowing small array measurements (Fig. 3.12). In the shown example the injection peaks are clearly visible. It is also possible to stretch the timeline of the displayed graph allowing a more detailed analysis of the measurements.

This program thus allows fast and reliable analysis of heat transfer resistance measurements on DNA and an easy way to visualize measurements using MIP/SIP sensors.

## Chapter 3 : Results & Discussion

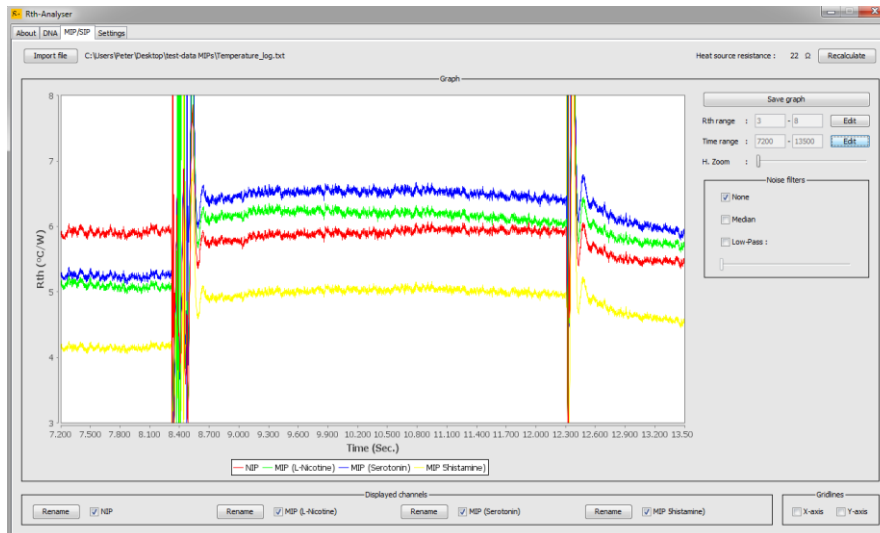


**Fig. 3.12.** MIP/SIP sheet of the Rth-Analyser program. As an example the evolution of the heat transfer resistance of an array containing a NIP, MIP(L-Nicotine), MIP(Serotonin) and MIP(Histamine) is shown. The first injection is a PBS solution containing L-Nicotine, Serotonin and Histamine. The second injection is a clean PBS solution.

## Chapter 3 : Results & Discussion

# Chapter 4: Conclusion

---

This study confirmed the possibility of using a method based on heat transfer resistivity to measure the concentration of a specific gene of interest, although further optimizations are necessary. The possibility to measure concentrations of a specific target sequence illustrates the potential of this technique to be used as a user-friendly alternative to determine the level of contamination with pathogens in food and drinking water production as well as clinical diagnostics and environmental studies. Moreover, this technique enables the calculation of the hybridization efficiency of a target DNA fragment to the probes.

The results showed that the current sensor has a hybridization efficiency of only 8 %. Increasing this is thus an obvious first step in optimizing the sensor. From literature it is known that lowering the probe density on the surface can increase the efficiency to over 90 %.<sup>(25)</sup> Two ways, involving only minor modifications to the existing protocol for attaching the probe DNA to the surface, should be evaluated. Lowering the amount of single stranded probe DNA that is exposed to the surface can be lowered is one way, but care must be taken that the layer of probe DNA attached to the surface remains homogeneous. Another method is to use double stranded DNA to attach the probes to the surface. After functionalization the dsDNA can be denatured using a 0.1 M NaOH solution, leaving only the single stranded probe DNA on the surface. Using dsDNA should theoretically assure an optimal distance between the individual probes. This kind of increase in efficiency could lead to a very significant decrease of the detection limit allowing the detection of much lower concentrations the currently possible using this technique. Therefore, these are easy and very promising modifications, which should be investigated further.

The software program developed during this study enhances the heat transfer method by enabling fast and consistent analysis of the measurement data. Java was used as the programming language because of past experience and its additional advantage of cross-platform compatibility, which means the same program can run unaltered on PC's, Mac's and Linux machines. The program can be easily converted from java to C++ if more speed is required or when it would ease integration into a larger program. The core of this program allows for the development of devices using the DNA based sensor that can automatically perform the measurement and generate the corresponding result. Adding a time dependant analysis component to the core would enable automating the measurement analysis for devices using MIP or SIP sensors. Integration into the measurement setup therefore allows for a further standardization of the heat transfer method used in this study.





# References

---

1. Morais VA, Haddad D, Craessaerts K, De Bock PJ, Swerts J, Vilain S, et al. PINK1 Loss of Function Mutations Affect Mitochondrial Complex I Activity via NdufA10 Ubiquinone Uncoupling. *Science*. 2014.
2. Martin ER, Lai EH, Gilbert JR, Rogala AR, Afshari AJ, Riley J, et al. SNPping away at complex diseases: analysis of single-nucleotide polymorphisms around APOE in Alzheimer disease. *American journal of human genetics*. 2000;67(2):383-94.
3. Vanden Bon N, van Grinsven B, Murib M, Yeap WS, Haenen K, De Ceuninck W, et al. Heat-transfer-based detection of SNPs in the PAH gene of PKU patients. *International Journal of Nanomedicine*. 2014;9(1):1629-40.
4. Schon EA, Bonilla E, DiMauro S. Mitochondrial DNA mutations and pathogenesis. *Journal of bioenergetics and biomembranes*. 1997;29(2):131-49.
5. Dunning AM, Healey CS, Pharoah PD, Teare MD, Ponder BA, Easton DF. A systematic review of genetic polymorphisms and breast cancer risk. *Cancer epidemiology, biomarkers & prevention : a publication of the American Association for Cancer Research, cosponsored by the American Society of Preventive Oncology*. 1999;8(10):843-54.
6. Hooper JW. The genetic map to theranostics. *MLO: medical laboratory observer*. 2006;38(6):22-3, 5.
7. Woo PCY, Lau SKP, Teng JLL, Tse H, Yuen KY. Then and now: use of 16S rDNA gene sequencing for bacterial identification and discovery of novel bacteria in clinical microbiology laboratories. *Clin Microbiol Infect*. 2008;14(10):908-34.
8. Lievens B, Claes L, Vanachter ACRC, Cammue BPA, Thomma BPHJ. Detecting single nucleotide polymorphisms using DNA arrays for plant pathogen diagnosis. *Fems Microbiol Lett*. 2006;255(1):129-39.
9. Ducey TF, Page B, Usgaard T, Borucki MK, Pupedis K, Ward TJ. A single-nucleotide-polymorphism-based multilocus genotyping assay for subtyping lineage I isolates of *Listeria monocytogenes*. *Applied and environmental microbiology*. 2007;73(1):133-47.
10. Juste A, Lievens B, Frans I, Klingeberg M, Michiels CW, Willems KA. Development of a DNA Array for the Simultaneous Detection and Identification of Sugar Thick Juice Bacterial Contaminants. *Food Anal Method*. 2011;4(2):173-85.
11. Peter H, Berggrav K, Thomas P, Pfeifer Y, Witte W, Templeton K, et al. Direct Detection and Genotyping of *Klebsiella pneumoniae* Carbapenemases from Urine by Use of a New DNA Microarray Test. *J Clin Microbiol*. 2012;50(12):3990-8.
12. Bakker HC, Switt AI, Cummings CA, Hoelzer K, Degoricija L, Rodriguez-Rivera LD, et al. A whole-genome single nucleotide polymorphism-based approach to trace and identify outbreaks linked to a common *Salmonella enterica* subsp. *enterica* serovar Montevideo pulsed-field gel electrophoresis type. *Applied and environmental microbiology*. 2011;77(24):8648-55.
13. Wenmackers S, Vermeeren V, vandeVen M, Ameloot M, Bijmens N, Haenen K, et al. Diamond-based DNA sensors: surface functionalization and read-out strategies. *Physica Status Solidi a-Applications and Materials Science*. 2009;206(3):391-408.
14. Vermeeren V, Wenmackers S, Daenen M, Haenen K, Williams OA, Ameloot M, et al. Topographical and functional characterization of the ssDNA probe layer generated through EDC-mediated covalent attachment to nanocrystalline diamond using fluorescence microscopy. *Langmuir : the ACS journal of surfaces and colloids*. 2008;24(16):9125-34.
15. Christiaens P, Vermeeren V, Wenmackers S, Daenen M, Haenen K, Nesladek M, et al. EDC-mediated DNA attachment to nanocrystalline CVD diamond films. *Biosens Bioelectron*. 2006;22(2):170-7.
16. Yang W, Auciello O, Butler JE, Cai W, Carlisle JA, Gerbi JE, et al. DNA-modified nanocrystalline diamond thin-films as stable, biologically active substrates. *Nature materials*. 2002;1(4):253-7.

## References

17. Kratka M, Kromka A, Ukraintsev E, Ledinsky M, Broz A, Kalbacova M, et al. Function of thin film nanocrystalline diamond-protein SGFET independent of grain size. *Sensor Actuat B-Chem.* 2012;166:239-45.
18. Ingebrandt S, Han Y, Nakamura F, Poghossian A, Schoning MJ, Offenhausser A. Label-free detection of single nucleotide polymorphisms utilizing the differential transfer function of field-effect transistors. *Biosens Bioelectron.* 2007;22(12):2834-40.
19. Poghossian A, Abouzar MH, Amberger F, Mayer D, Han Y, Ingebrandt S, et al. Field-effect sensors with charged macromolecules: Characterisation by capacitance-voltage, constant-capacitance, impedance spectroscopy and atomic-force microscopy methods. *Biosens Bioelectron.* 2007;22(9-10):2100-7.
20. Vagin MY, Karyakin AA, Hianik T. Surfactant bilayers for the direct electrochemical detection of affinity interactions. *Bioelectrochemistry.* 2002;56(1-2):91-3.
21. Poghossian A, Abouzar MH, Sakkari M, Kassab T, Han Y, Ingebrandt S, et al. Field-effect sensors for monitoring the layer-by-layer adsorption of charged macromolecules. *Sensor Actuat B-Chem.* 2006;118(1-2):163-70.
22. van Grinsven B, Vanden Bon N, Strauven H, Grieten L, Murib M, Monroy KL, et al. Heat-transfer resistance at solid-liquid interfaces: a tool for the detection of single-nucleotide polymorphisms in DNA. *ACS nano.* 2012;6(3):2712-21.
23. Ambia-Garrido J, Vainrub A, Pettitt BM. A model for Structure and Thermodynamics of ssDNA and dsDNA Near a Surface: a Coarse Grained Approach. *Computer physics communications.* 2010;181(12):2001-7.
24. Bers K, van Grinsven B, Vandenryt T, Murib M, Janssen W, Geerets B, et al. Implementing heat transfer resistivity as a key element in a nanocrystalline diamond based single nucleotide polymorphism detection array. *Diam Relat Mater.* 2013;38:45-51.
25. Peterson AW, Heaton RJ, Georgiadis RM. The effect of surface probe density on DNA hybridization. *Nucleic acids research.* 2001;29(24):5163-8.
26. Ravan H, Kashanian S, Sanadgol N, Badoei-Dalfard A, Karami Z. Strategies for optimizing DNA hybridization on surfaces. *Analytical biochemistry.* 2014;444:41-6.
27. Vainrub A, Pettitt BM. Coulomb blockage of hybridization in two-dimensional DNA arrays. *Physical review E, Statistical, nonlinear, and soft matter physics.* 2002;66(4 Pt 1):041905.
28. Janssens SD, Drijkoningen S, Saitner M, Boyen HG, Wagner P, Larsson K, et al. Evidence for phase separation of ethanol-water mixtures at the hydrogen terminated nanocrystalline diamond surface. *The Journal of chemical physics.* 2012;137(4):044702.
29. Wang X, Ruther RE, Streifer JA, Hamers RJ. UV-induced grafting of alkenes to silicon surfaces: photoemission versus excitons. *Journal of the American Chemical Society.* 2010;132(12):4048-9.
30. Wenmackers S, Pop SD, Roodenko K, Vermeeren V, Williams OA, Daenen M, et al. Structural and optical properties of DNA layers covalently attached to diamond surfaces. *Langmuir : the ACS journal of surfaces and colloids.* 2008;24(14):7269-77.
31. Guo X, Gorodetsky AA, Hone J, Barton JK, Nuckolls C. Conductivity of a single DNA duplex bridging a carbon nanotube gap. *Nature nanotechnology.* 2008;3(3):163-7.
32. Lenz M, Striedl U, Fröhler. SMD Packages. Thermal resistance, theory and practice. Released by Infineon Technologies AG, Munich, Germany. 2000.
33. Peeters M, Csipai P, Geerets B, Weustenraed A, van Grinsven B, Thoelen R, et al. Heat-transfer-based detection of L-nicotine, histamine, and serotonin using molecularly imprinted polymers as biomimetic receptors. *Analytical and bioanalytical chemistry.* 2013;405(20):6453-60.
34. Eersels K, van Grinsven B, Ethirajan A, Timmermans S, Jimenez Monroy KL, Bogie JF, et al. Selective identification of macrophages and cancer cells based on thermal transport through surface-imprinted polymer layers. *ACS applied materials & interfaces.* 2013;5(15):7258-67.

# Supplemental Information

---

## Articles

### Heat transfer resistance as a tool to quantify hybridization efficiency of DNA on a nanocrystalline diamond surface.

P. Cornelis<sup>1,†</sup>, T. Vandenryt<sup>1,2,†</sup>, G. Wackers<sup>1</sup>, E. Kellens<sup>1,3</sup>, P. Losada-Pérez<sup>1</sup>, R. Thoelen<sup>1,3</sup>, W. De Ceuninck<sup>1,3</sup>, K. Eersels<sup>1,\*</sup>, S. Drijkoningen<sup>1</sup>, K. Haenen<sup>1</sup>, M. Peeters<sup>1,3</sup>, B. van Grinsven<sup>1,4</sup>, P. Wagner<sup>1,3</sup>

<sup>1</sup> Hasselt University, Institute for Materials Research, Wetenschapspark 1, B-3590 Diepenbeek, Belgium

<sup>2</sup> XIOS University College, Department of Applied Engineering, Agoralaan – Building H, B-3590 Diepenbeek, Belgium

<sup>3</sup> IMOMEC, Wetenschapspark 1, B-3590 Diepenbeek, Belgium

<sup>4</sup> Maastricht Science Programme, Maastricht University, Post Office Box 616, 6200 MD Maastricht, Netherlands

<sup>†</sup> Authors contributed equally to this work

\* Author to whom correspondence should be addressed; E-Mail: Kasper.Eersels@uhasselt.be; Tel.: +32-11-26-88xx; Fax: +32-11-26-8813

#### Abstract

In this article, we report on a label-free real-time method based on heat transfer resistivity for thermal monitoring of DNA denaturation and its potential to quantify DNA fragments with a specific sequence of interest. Probe DNA, consisting of a 36-mer fragment was covalently immobilized on a nanocrystalline diamond surface, created by chemical vapor deposition on a silicon substrate. Various concentrations of full matched 29-mer target DNA fragments were hybridized with this probe DNA. We observed that the change in heat transfer resistance upon denaturation depends on the concentration of target DNA used during the hybridization, which allowed to determine the dose response curve. Therefore, these results illustrate the potential of this technique to quantify the concentration of a specific DNA fragment and to quantify the hybridization efficiency to its probe.

Submitted to "Diamond and Related Materials" on April, 4, 2014.

*Communication*

## Array formatting of the heat-transfer method (HTM) for the detection of small organic molecules by molecularly imprinted polymers

G. Wackers<sup>1,†</sup>, T. Vandenryt<sup>1,†</sup>, P. Cornelis<sup>1</sup>, E. Kellens<sup>1,2</sup>, R. Thoelen<sup>1,2</sup>, W. De Ceuninck<sup>1,2,\*</sup>, P. Losada-Pérez<sup>1,2</sup>, B. van Grinsven<sup>1,2,3</sup>, M. Peeters<sup>1,2</sup>, and P. Wagner<sup>1,2</sup>

<sup>1</sup> Hasselt University, Institute for Materials Research, Wetenschapspark 1, B-3590 Diepenbeek, Belgium

<sup>2</sup> IMEC vzw – Division IMOMECE, Wetenschapspark 1, B-3590 Diepenbeek, Belgium

<sup>3</sup> Maastricht Science Programme, Maastricht University, 6200 MD Maastricht, Netherlands

<sup>†</sup> Authors contributed equally to this work

\* Author to whom correspondence should be addressed; E-Mail: Ward.Deceuninck@uhasselt.be; Tel.: +32-11268872; Fax: +32-11268899

*Received: / Accepted: / Published:*

---

**Abstract:** In this work we present the first steps towards a molecularly imprinted polymer (MIP) based biomimetic sensor array for the detection of small organic molecules via the heat-transfer method (HTM). HTM relies on the change in thermal resistance upon binding of the target molecule to the MIP-type receptor. A flow-through sensor cell was developed, which is segmented into four quadrants with a volume of 2.5  $\mu$ L each, allowing four measurements to be done simultaneously on a single substrate. Verification measurements were conducted, in which all quadrants received a uniform treatment and all four channels exhibited a similar response. Subsequently, measurements were performed in quadrants, which were functionalized with different MIP particles. Each of these quadrants was exposed to the same buffer solution, spiked with different molecules, according to the MIP under analysis. With the flow cell design we could discriminate between similar small organic molecules and observed no significant cross-selectivity. Therefore, the MIP array sensor platform with HTM as a readout technique, has the potential to become a low-cost analysis tool for bioanalytical applications.

**Keywords:** heat-transfer method (HTM); molecularly imprinted polymers (MIPs); serotonin; histamine; L-nicotine, array format.

---

## Auteursrechtelijke overeenkomst

Ik/wij verlenen het wereldwijde auteursrecht voor de ingediende eindverhandeling:

**Heat transfer resistance as a tool to quantify hybridization efficiency of DNA on a nanocrystalline diamond surface**

Richting: **master in de biomedische wetenschappen-bio-elektronica en nanotechnologie**

Jaar: **2014**

in alle mogelijke mediaformaten, - bestaande en in de toekomst te ontwikkelen - , aan de Universiteit Hasselt.

Niet tegenstaand deze toekenning van het auteursrecht aan de Universiteit Hasselt behoud ik als auteur het recht om de eindverhandeling, - in zijn geheel of gedeeltelijk -, vrij te reproduceren, (her)publiceren of distribueren zonder de toelating te moeten verkrijgen van de Universiteit Hasselt.

Ik bevestig dat de eindverhandeling mijn origineel werk is, en dat ik het recht heb om de rechten te verlenen die in deze overeenkomst worden beschreven. Ik verklaar tevens dat de eindverhandeling, naar mijn weten, het auteursrecht van anderen niet overtreedt.

Ik verklaar tevens dat ik voor het materiaal in de eindverhandeling dat beschermd wordt door het auteursrecht, de nodige toelatingen heb verkregen zodat ik deze ook aan de Universiteit Hasselt kan overdragen en dat dit duidelijk in de tekst en inhoud van de eindverhandeling werd genotificeerd.

Universiteit Hasselt zal mij als auteur(s) van de eindverhandeling identificeren en zal geen wijzigingen aanbrengen aan de eindverhandeling, uitgezonderd deze toegelaten door deze overeenkomst.

Voor akkoord,

**Cornelis, Peter**

Datum: **10/06/2014**